REPORT

Modeling position specific carbon isotopologue fractionation of thermogenic propane and precursors

Biao Jin[1,2,3,4,*] **and Ping'an Peng**[1,2,3,*]

*Correspondence: jinbiao@gig.ac.cn(B.J.); pinganp@gig.ac.cn(P.P.)

Received: October 31, 2023; Accepted: February 24, 2024; Published Online: March 2, 2024; https://doi.org/10.59717/j.xinn-geo.2024.100054

GRAPHICAL ABSTRACT

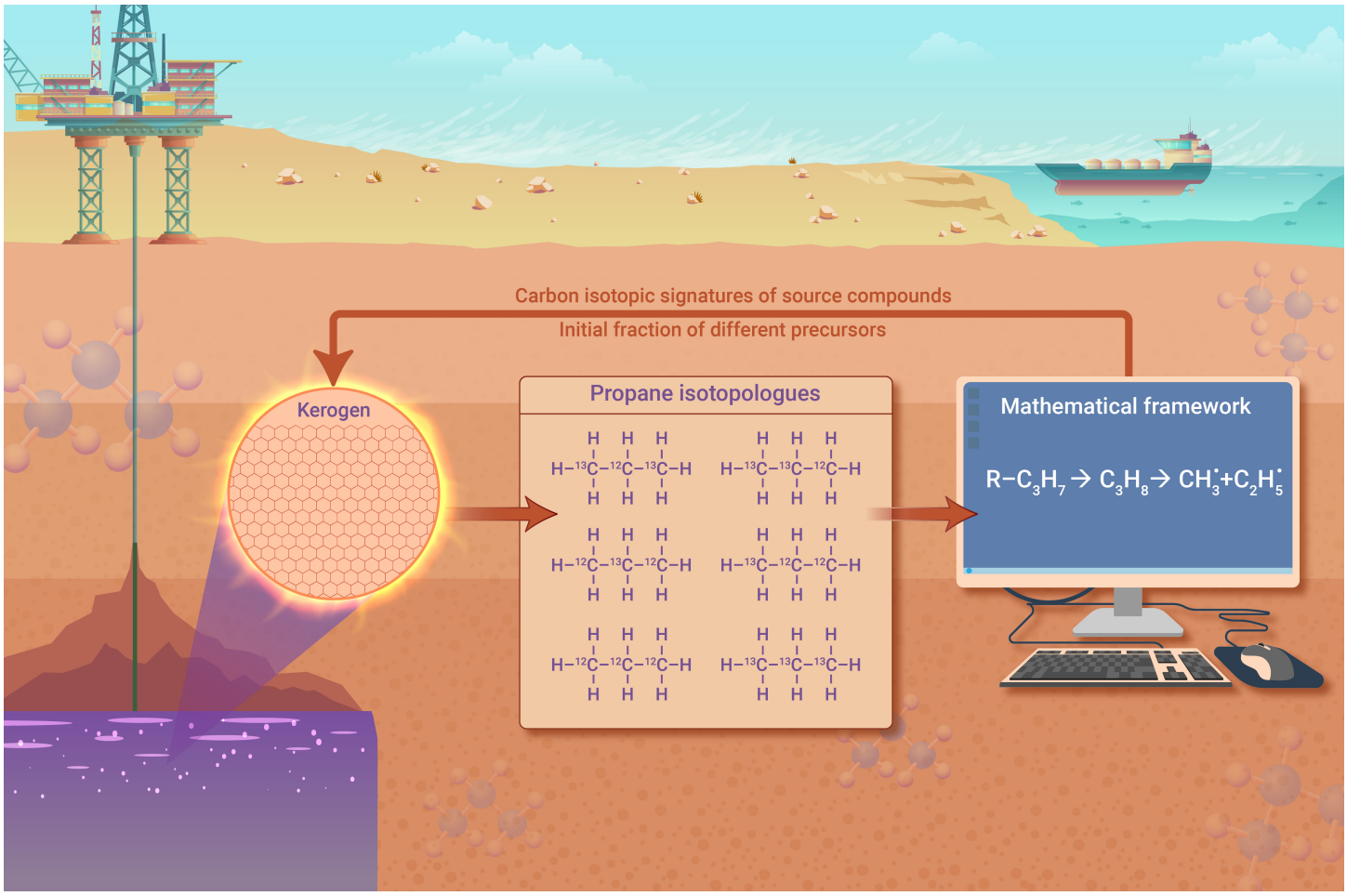

PUBLIC SUMMARY

- A mathematical framework to describe carbon isotopic evolution of thermogenic propane and its precursors.
- Initial fraction and isotopic signatures of different propane precursors are quantified by our model.
- Source compounds distribution could impact position specific carbon isotopic signals of thermogenic propane.

REPORT

www.the-innovation.org/geoscience

Modeling position specific carbon isotopologue fractionation of thermogenic propane and precursors

Biao Jin[1,2,3,4,*] **and Ping'an Peng**[1,2,3,*]

[1]State Key Laboratory of Organic Geochemistry, Guangzhou Institute of Geochemistry, Chinese Academy of Sciences, Guangzhou 510640, China
[2]CAS Center for Excellence in Deep Earth Science, Guangzhou 510640, China
[3]University of Chinese Academy of Sciences, Beijing 100049, China
[4]Guangdong Provincial Key Laboratory of Environmental Protection and Resources Utilization, Guangzhou 510640, China
*Correspondence: jinbiao@gig.ac.cn(B.J.); pinganp@gig.ac.cn(P.P.)

Received: October 31, 2023; Accepted: February 24, 2024; Published Online: March 2, 2024; https://doi.org/10.59717/j.xinn-geo.2024.100054

Citation: Jin B. and Peng P. (2024). Modeling position specific carbon isotopologue fractionation of thermogenic propane and precursors. The Innovation Geoscience **2(1)**: 100054.

Position specific isotope analysis (PSIA) of thermogenic propane allows to track carbon isotopic compositions at different molecular positions, and thus providing new evidence to investigate propane's origin, fate, and mechanisms of formation. However, the link between observed $\delta^{13}C$ PSIA signals of propane and carbon isotopologue signatures of precursors in source organics still remains unclear, and understanding the underlying mechanisms requires a more sophisticated model. Here we developed a mathematical framework to simulate position specific carbon isotopologues of propane and its precursors based on mechanistic understanding of thermogenic propane's bond-cleavage pathways. Besides, our model also allows integrating multiple signals including temperature, and isotopic characteristics of source compounds. Our model is validated by precisely reproducing propane's experimental PSIA data obtained during cracking of different kerogens, and also correctly quantified the initial carbon isotopic signatures and the initial fraction of the different precursors in the source materials. Our model allows to include more complex reaction mechanisms to elucidate unknown reaction pathways, and could also guide and optimize future experimental studies to test different hypothesis.

INTRODUCTION

Thermogenic degradation of sedimentary organic matter could release natural gas hydrocarbons, including methane, ethane, propane, and butane isomers.[1-5] Meantime, natural gas molecules also degrade via abiotic thermal degradation and/or biological reactions.[6,7] Propane is the shortest hydrocarbon containing two distinct carbon positions. The central and terminal carbon atoms carry isotopic signatures from precursors, and also could undergo different bond-cleavage pathways.[8-10] For instance, the difference on isotopic signatures between central and terminal carbon positions of propane could indicate the temperature of a basin or the extent of thermal cracking.[11-13] For these reasons, development of position-specific isotope analysis (PSIA) measurements allows to track isotopic compositions at different molecular positions, and thus providing new evidence to investigate propane's origin, fate, and mechanisms of formation.[9,12,14]

Given thermogenic propane's position-specific carbon isotopic evolution is associated with both thermodynamic processes and kinetic reaction networks, mechanistic interpretation of propane's PSIA signals is of primary importance, and therefore requiring mathematical frameworks. Conventional kinetic models were developed in previous studies to reproduce isotopic trends of thermogenic hydrocarbons, indicating that carbon isotope fractionation exclusively occurs at C–C bond cleavage positions.[15-17] The reactive carbon atoms of propane isotopically fractionate while other carbon atoms inherit isotope compositions of precursors.[16,18] Moreover, even $\delta^{13}C$ PSIA signals of thermogenic propane is dependent on source materials characteristics, how and on what extend these parameters of precursors will influence propane's carbon PSIA patterns still remains unclear. Thus, resolving the isotopomers' signature of thermogenic propane definitely require more sophisticated models[19-22] in order to understand position specific isotope fractionation of thermogenic propane.

The ultimate goal of our study is to establish a mathematical framework to simulate position specific carbon isotopologue fractionation of thermogenic propane and its precursors. To this end, it is hypothesized that two different propane precursors occur in source materials, which are associated with C-C bond cleavage at propane's terminal and central carbon positions (see Figure 1). Both initial fraction and carbon isotopic signatures of different precursors are allowed to be considered and defined in our model as input parameters. The specific tasks are (i) to build a mathematical framework to model reaction network of position specific isotopologues of both propane and its precursors during different cracking stages; (ii) to validate the model using experimental data; and (iii) to quantify initial fraction and carbon isotopic signatures of individual precursor in different kerogen.

MATERIALS AND METHODS

Reaction pathways and isotopologue speciation

Mathematical expression of propane isotopologues reaction kinetics is described by tracking bond-cleavage pathways during both formation and degradation of propane isotopologues. The reaction pathway is described as follow:

$$R-C_3H_7 \rightarrow C_3H_8 \rightarrow CH_3^{\bullet} + C_2H_5^{\bullet} \quad (1)$$

where the precursor, $R\text{-}C_3H_7$, is forming propane via two pathways by cleaving one terminal carbon atom or one central carbon atom in propane molecules away from the two precursors, respectively (see pathway A and B in Figure1). Pathway A and B are simultaneously forming different propane isotopologues, and therefore influencing terminal and central carbon isotopic compositions of propane yield during thermolysis reactions. The initial relative abundances of the position-specific carbon isotopologues of the propane's precursor (i.e. R–C–C_3) for pathway A or B are defined as:

$$A_j = X_{^{13}C}^{a} \cdot X_{^{12}C}^{4-a} \quad (2)$$

$$B_j = Y_{^{13}C}^{b} \cdot Y_{^{12}C}^{4-b} \quad (3)$$

Considering the occurrence of three carbon isotopes in propane to be cleaved from the precursor (R–C–C_3), as well as the carbon isotope at neighboring bond cleavage positions of the precursor. Here we simplified the precursor isotopologues into a molecule containing four carbon atoms (C–C_3). Notably, every carbon atom in C–C_3 is playing a unique role in our model, contributing to position-specific carbon isotope fractionation during bond-cleavage reactions. For this reason each isotopologue is defined in a position-specific manner in Eqs 2 and 3. Specifically, A_j and B_j are the relative abundances of the j^{th} position-specific isotopologue containing a specific number of ^{13}C isotopes (i.e. *"a"*) out of total 4 carbon atoms and a specific number of ^{13}C isotopes (i.e. "*b*") out of total 4 carbon atoms for pathway A and B, respectively. X and Y are determined by using initial carbon isotope ratios in different precursors that are forming propane via pathway A and B, respectively.

As it is demonstrated in Figure 1, the formed propane isotopologues might carry different carbon isotopic compositions at both central and side carbon positions. These propane isotopologues could break down by cleaving one C-C bond, and thus leading to carbon isotope fractionation at both central and terminal positions. The bond cleavage pathways of propane isotopologues are described in Figure 1C.

Kinetic isotope effect during cleavage of C–C bond

Isotopologues of different propane precursors, R–C_a and R–C_b, may include

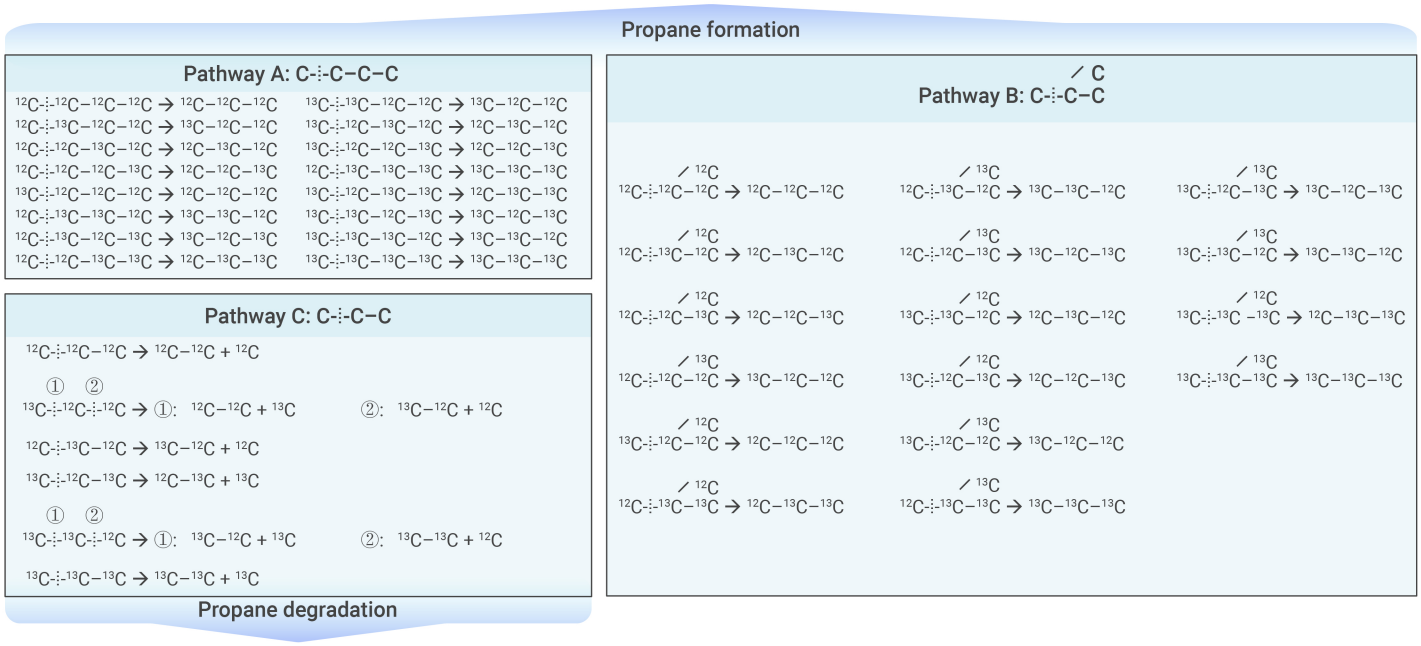

Figure 1. Reaction network and bond-cleavage pathways of thermogenic propane and its precursors' isotopologues Pathway A: terminal carbon cleaved from precursor A; Pathway B: central carbon cleaved from precursor B; Pathway C: possible bond cleavage pathways for propane degradation. The number indicates two concurrent bond-cleavage pathways.

reactive C–C bonds with different carbon isotopic compositions, which are ^{12}C–^{12}C, ^{13}C–^{12}C, ^{12}C–^{13}C, and ^{13}C–^{13}C, respectively. Following a first-order kinetic, the reaction rates during cleavage of different C–C bonds are:

$$ {}^{j}r_A = -k_{precursor} \cdot (a_A)^h \cdot {}^{j}C_A \tag{4} $$

$$ {}^{j}r_B = -k_{precursor} \cdot (a_B)^i \cdot {}^{j}C_B \tag{5} $$

where ${}^{j}r$ is the reaction rate for the j^{th} position-specific isotopologue, R-C_4, which is associated with pathway A or B, ${}^{j}C$ is the concentration of the j^{th} position-specific isotopologue, and a_A and a_B are the fractionation factors (i.e. k_{13C}/k_{12C}) at reactive positions for pathway A and B, respectively. The exponents h and i indicate the number of ^{13}C isotopes at a bond-cleavage position, and this number could vary from 0 to 2.

In our example the pyrolysis temperature (i.e. T_t) increases at a constant rate (i.e. r_{temp}). The rate constant at a specific temperature (i.e. k_t) is described by Arrhenius equation:

$$ k_t = k_0 \cdot \exp\left\{\frac{E_a}{R}\left(\frac{1}{T_0} - \frac{1}{T_t}\right)\right\} \tag{6} $$

$$ \frac{dT_t}{dt} = r_{temp} \tag{7} $$

The position specific propane isotopologue, C_a-C_b-C_a , could further react by cleaving one C_a-C_b bond, leading to position specific isotope fractionation of propane. Following a first-order kinetic, the consumption rate of the k_{th} propane isotopologue are:

$$ {}^{k}r_{propane} = -k_{propane} \cdot (a_a)^m \cdot (a_b)^n \cdot {}^{k}C_{propane} \tag{8} $$

where ${}^{k}r$ is the reaction rate for the k^{th} position-specific propane isotopologue, C_a-C_b-C_a, which is associated with pathway A or B; C_k is the concentration of the k^{th} position-specific propane isotopologue, and a_a and a_b are the fractionation factors (i.e. k_{13C}/k_{12C}, α<1) at reactive positions side and central carbon atoms, respectively. The exponent m and n indicate the number of ^{13}C isotope at a reactive C_a-C_b bond, ranging from 0 to 1. The first order reaction rate, $k_{propane}$, varies with reaction time and is correlated with reaction temperature by eqs 6 and 7.

The isotope fractionation between the total carbon in the cleaved radical and the one in the precursor can be calculated at any temperatures based on the following equation developed in the previous study:[16]

$$ a_t = \frac{k^*}{k} = \frac{A_f^*}{A_f} \cdot \exp\left\{-\frac{\Delta E_a}{RT_t}\right\} \tag{9} $$

The fractionation factor a at an increasing temperature for methyl (i.e. a_a), ethyl (i.e. a_b) and propyl radicals (i.e. a_A and a_B in eqs 4 and 5), A_f^*/A_f and ΔE_a are the fitted prefactor ratios and activation energy differences, respectively. These parameters (see Table S1 in supplementary information) were adopted from a previous study[16] and used as model input parameters to calculate temperature-dependent carbon isotope fractionation factors for propane formation and thermal degradation, respectively.

Reaction kinetics and position specific isotope ratio

The reaction rate of a specific propane precursor's isotopologue via pathway A or B depends on the corresponding carbon isotopic compositions of reactive C-C bonds, and consumption rates of the precursor via pathway A or B is the summation of the relevant isotopologue-specific reaction rates (eqs 4 and 5). The mathematical expressions are given as:

$$ \frac{dC_{A,precursor}}{dt} = -\sum_{j=1}^{16} {}^{j}r_A \tag{10} $$

$$ \frac{dC_{B,precursor}}{dt} = -\sum_{j=1}^{16} {}^{j}r_B \tag{11} $$

where C refers to temporal concentration of different propane precursors; ${}^{j}r$ is the reaction rate for the j^{th} position-specific isotopologue as defined in eqs 4 and 5.

A specific propane isotopologue could be formed by different precursors via pathways A and/or B (see Figure 1). Simultaneously, the propane isotopologues could break down at different rates according to their intrinsic carbon isotopic compositions. This kinetic process is described in eq12. Concerning temporal trend of propane concentrations ($C_{propane}$), it is an interplay between formation rates and consumption rates of all the propane isotopologues (${}^{k}C_{propane}$) as described in eq13.

$$ \frac{d^{k}C_{propane}}{dt} = +\sum_{j=1}^{2} {}^{j}r_A + \sum_{j=1}^{2} {}^{j}r_B - \sum_{k=1}^{t} {}^{k}r_{propane} \tag{12} $$

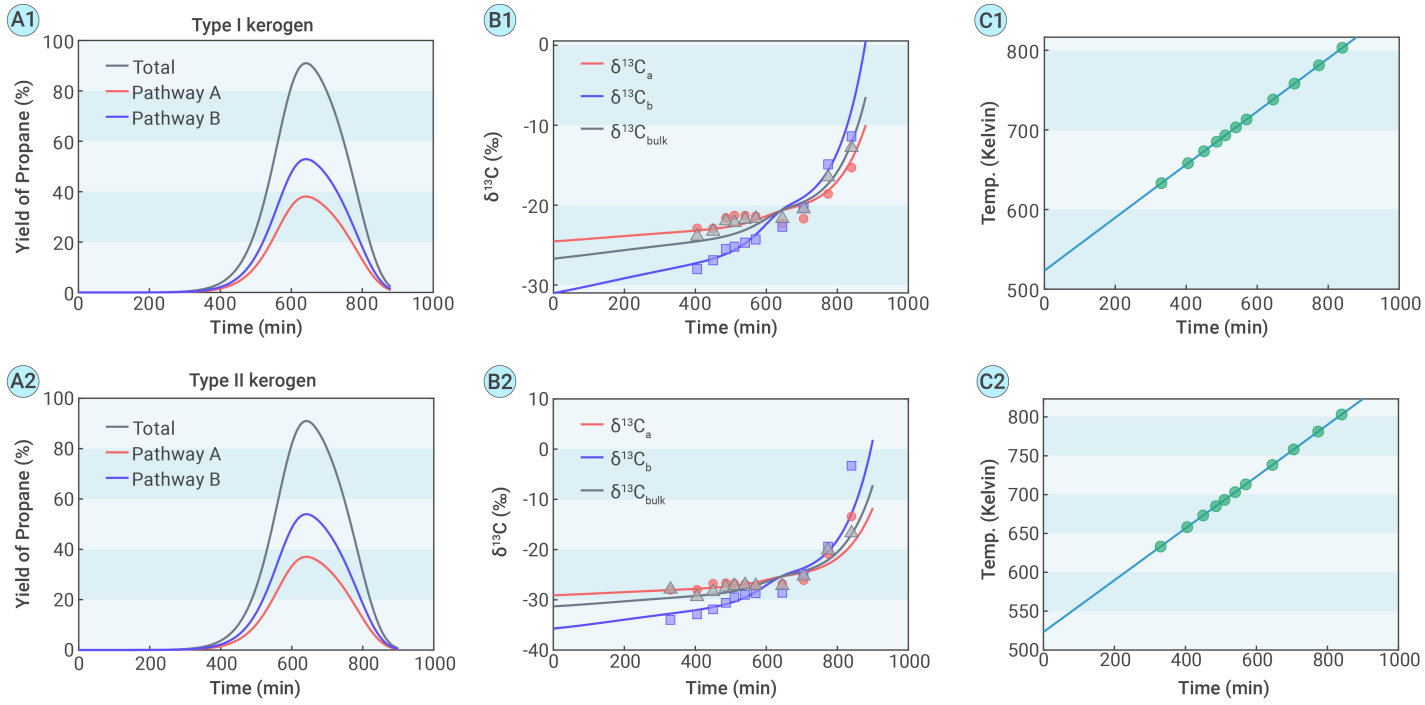

Figure 2. Temporal trends of propane production and associated compound specific and position specific carbon isotope fractionation during thermolysis of Type I and II kerogens The symbols represent the experimental data adopted in the previous study.[9] The solid lines are the model simulated results.

$$C_{propane,t} = \sum_{k=1}^{16} {}^{k}C_{propane,t} \quad (13)$$

The propane carbon isotopologues reaction kinetics and network during formation and thermal degradation are described using the above mentioned system of differential equations. Notably, "*j* " is only up to 2 due to the fact that there are two precursor-isotopologues (C-C_3) forming a specific propane isotopologue via Pathway A or B as it is demonstrated in Figure1. These equations are programmed and solved using ODE solver of Matlab software. The calculated propane isotopologues' temporal concentrations are later used to compute position specific and bulk carbon isotopic ratios of propane. The position specific carbon isotopic ratios (R_a and R_b) and the bulk carbon isotopic ratios ($R_{propane}$) of propane are computed by counting total number of ^{13}C and ^{12}C isotopes.[23,24]

$$R_{a,t} = \frac{\mathrm{tot}(^{13}C_a)}{\mathrm{tot}(^{12}C_a)} = \frac{\sum_{k=1}^{6} u \cdot {}^{k}C_{propane,t}}{\sum_{k=1}^{6} (2-u) \cdot {}^{k}C_{propane,t}} \quad (14)$$

$$R_{b,t} = \frac{\mathrm{tot}(^{13}C_b)}{\mathrm{tot}(^{12}C_b)} = \frac{\sum_{k=1}^{6} v \cdot {}^{k}C_{propane,t}}{\sum_{k=1}^{6} (1-v) \cdot {}^{k}C_{propane,t}} \quad (15)$$

$$R_{propane,t} = \frac{2}{3} \cdot R_{a,t} + \frac{1}{3} \cdot R_{b,t} \quad (16)$$

"*u*" indicates a total number of ^{13}C isotopes at the two terminal carbon positions ($u \leq 2$) of different propane iostopologues; "*v*" indicates a total number of ^{13}C isotopes ($v \leq 1$) at the central carbon position of different propane isotopologues.

The calculated carbon isotopic ratios (R) are referenced to the isotope ratios of the standard materials (R_{std}) and are expressed in delta notation ($\delta^{13}C$):

$$\delta^{13}C_t = \frac{R_t}{R_{std}} - 1 \ [‰] \quad (17)$$

Experimental data. The carbon isotopic data of thermogenic propane were obtained for different types of kerogens during pyrolysis simulations, which was reported in a recent experimental study.[11] The characteristics of the target kerogens were summarized in Table S2. Specifically, the two kerogens have different organic contents (i.e. Type II <Type I). The experimental setup was heated at a constant rate (i.e. 20 ℃/hour), and the temporal compound specific and position specific carbon isotopic ratios of propane yields were analyzed. The detailed description of experimental protocols and analytical approaches are available in the previous publication.[11] Briefly, the relevant experimental parameters and data sets adopted for our modelling studies were summarized in Table S2-S4.

RESULTS

Modeling carbon isotopologues of propane and precursors

Our model was applied to simulate carbon isotopic fractionation of propane yields. As shown in Figure 2 (b1 and b2) the carbon isotopic compositions of terminal (i.e. $\delta^{13}C_a$, red lines and markers) and central carbon (i.e. $\delta^{13}C_b$, blue lines and markers) atoms and bulk propane (i.e. $\delta^{13}C_{bulk}$, dark lines and markers) were precisely captured by our model. The mean squared error (MSE) were calculated to evaluate the match between the simulated results and the experimental data (see Table S5 and S6). The $\delta^{13}C_a$ values increased from -22.9‰ to -15.3‰, from -27.9‰ to -13.4‰ for Type I and II kerogen, respectively. The $\delta^{13}C_b$ values increased from -28.0 ‰ to -11.4 ‰, from -34.0‰ to -3.3‰ for Type I and II kerogen, respectively. The $\delta^{13}C_{bulk}$ values are dependent on contributions of both pathways, and increased from -23.9‰ to -12.8‰, from -27.9‰ to -16.7‰ for Type I and II kerogen, respectively. At early stage carbon isotopic compositions of propane were predominantly influenced by cracking Type I and Type II kerogens through both pathway A and B, leading to preferential cleavage of ^{12}C-containing bonds as well as yield of isotopically lighter propane isotopologues (see Figure 1).

Along with the elevated temperature destruction of propane molecules becomes increasingly more important, which preferentially cleaves ^{12}C-containing bonds in propane molecules, and therefore resulting in stronger isotope fractionation at central carbon position due to "diluted" carbon isotopic effects at two terminal carbon positions. Thus, the temporal $\delta^{13}C_b$ values are gradually approaching the $\delta^{13}C_a$ curves (see Figure 2 panel b1 and b2). At late stage breakdown of propane molecules becomes predominant, and therefore leading to a sharp increase of both bulk and position specific carbon isotopic ratios. Our model precisely reproduced carbon isotopic trend

Table 1. The model predicted initial parameters for propane's precursors in different kerogens.

Parameters	Type I Kerogen	Type II Kerogen
$\delta^{13}C_{precursor,A}$ [‰]	-16.50	-19.44
$\delta^{13}C_{precursor,B}$ [‰]	-24.00	-29.75
$\delta^{13}C_{bulk,\ measured*}$ [‰]	-20.70	-25.53
$\delta^{13}C_{bulk,\ predicted}$ [‰]	-20.86	-25.30
$f_{A,0}$ [%]	41.85	40.70
$f_{B,0}$ [%]	58.15	59.30

*: data is obtained from the previous study[11]

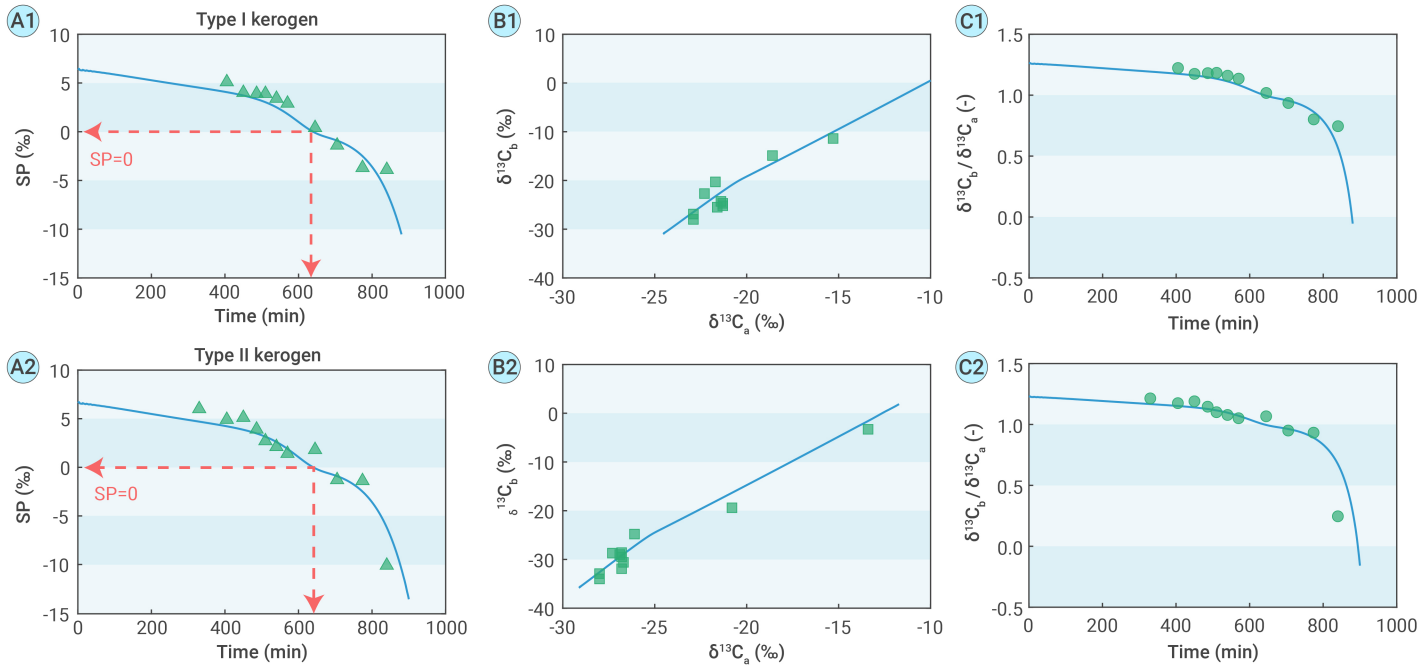

Figure 3. Temporal trend of site preference (SP) values, and $\delta^{13}C_a$ and $\delta^{13}C_b$ correlations of propane released during cracking of Type I and II kerogens The symbols represent the experimental data adopted in the previous study.[9] The solid lines are the model simulated results.

of propane at different reaction stages for both Type I and II kerogens. Moreover, the amount of released propane molecules relies on both formation and destruction processes, which is expressed as a percentage of actual propane yields over the total amount of extractable propane in a specific kerogen sample. The propane yields exclusively by pathway A or B could be quantified by our model (i.e. red lines or blue lines in Figure2 panel a1). The peak of propane yields appears when central carbon isotopic ratios are equivalent with the values at terminal carbon positions (i.e. propane site preference (SP) value equals zero). Besides, the temperature variations during cracking are also considered in our model in order to simulate temperature-dependent reaction rate constants and carbon isotopic fractionation factors (see eqs 6 and 9) at each time step. Hence, the simulated multiple signals, including propane yields, position specific and bulk carbon isotopic ratios, and temperatures, agree well with the experimental data. Importantly, this validated modelling approach could provide mechanistic predictions of position specific carbon isotopic evolution of thermogenic propane, and also the contributions of the two concurrent pathways are dependent on the initial fraction of the precursors (see Table 1). The relevant results will be discussed in detail in the following paragraphs.

Interpretation of reaction mechanisms and source characteristics

The simulated position specific carbon isotopic ratios of propane (i.e. $\delta^{13}C_a$ and $\delta^{13}C_b$ in Figure2, panel b1 and b2) were used to calculate temporal SP values (see Figure 3, panel a1 and a2) as well as to explore the $\delta^{13}C_b$ and $\delta^{13}C_a$ correlations (see Figure 3, panel b1, b2, c1 and c2). The model simulated values well captured the temporal experimental data. Generally, propane yields are following two main stages: i) the two concurrent pathways are competing until the SP values approach zero; ii) propane destruction process becomes predominant and alter the temporal trend of SP values. Notably, the two stages are clearly visualized and characterized in Figure 3 (b1 and b2), where the slopes shift significantly at the time that $\delta^{13}C_a$ and $\delta^{13}C_b$ values become identical.

Kerogens are characterized and classified according to their initial fraction of long-chain aliphatic hydrocarbons and side-chain hydrocarbons. These features of kerogens might influence observed intra-molecular carbon isotopic compositions of thermogenic propane. Indeed, the observed molecular and intra-molecular carbon isotopic ratios of propane are an interplay between the above mentioned concurrent reaction pathways (see pathway A and B in Figure 1), where Pathway B preferentially produces propane molecules containing ^{12}C at central carbon position, while Pathway A preferentially produces propane molecules containing ^{12}C at terminal carbon positions. Besides, destruction of propane molecules at late reaction stage is increasingly playing an important role by preferentially cleaving ^{12}C-containing C-C bonds of the produced propane, gradually elevating both molecular and position specific carbon isotopic ratios.

Our model takes into account propane yields via different reaction pathways as well as the initial characteristics of different precursors, and therefore providing mechanistic interpretation of position specific carbon isotopic

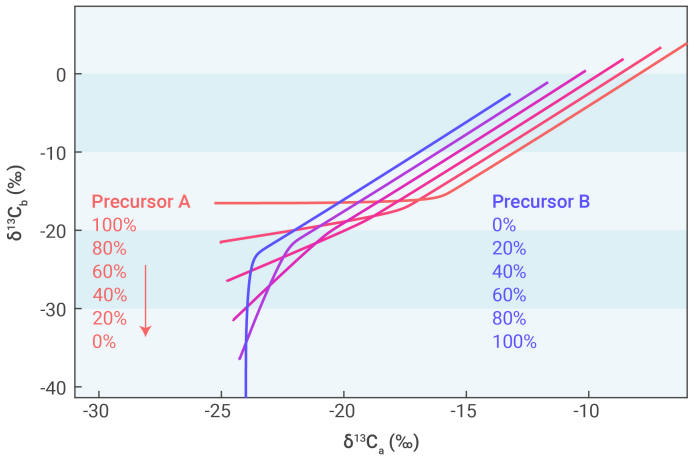

Figure 4. Simulated $\delta^{13}C_a$ and $\delta^{13}C_b$ correlations of propane released during cracking of Type I kerogen containing different fraction of precursor A and precursor B The darker lines stand for higher initial content of precursor A but lower content of precursor B in kerogen.

evolution of propane. At early time carbon isotopic compositions at central carbon position (i.e. $\delta^{13}C_b$) vary along with C-C bond cleavage from the precursor (i.e. pathway B). The produced propane molecules are still carrying initial carbon isotopic signatures of precursor B in their terminal carbon positions, and later these propane molecules are mixing with the ones formed via pathway A. Similarly, carbon isotope fractionation at terminal carbon positions (i.e. $\delta^{13}C_a$) is caused by C-C bond cleavage from alkanes (i.e. pathway A). The central carbon atoms of the produced propane via pathway A are carrying the original carbon isotopic signature of precursor A. Thus, the measured position specific carbon isotopic ratios of propane (i.e. $\delta^{13}C_b$ and $\delta^{13}C_a$) are influenced by both reaction pathways, where mixing of propane isotopologues released via the two reaction pathways together with bond-cleavage induced apparent carbon isotope effects are contributing to temporal variation of the observed $\delta^{13}C_b$ and $\delta^{13}C_a$ patterns of thermogenic propane. Our model describes the above mentioned mechanisms and processes by tracking evolution of individual propane and its precursor's isotopologue.

The observed position-specific carbon isotopic profiles of propane were influenced by both original carbon isotopic signatures and initial fraction of precursor A and B. Here, our model could quantify the initial parameters of the two precursors. Specifically, the initial fraction and carbon isotopic signatures of different precursors are defined as model input parameters, and these parameters are optimized and quantified by reproducing the observed position-specific carbon isotopic trends of thermogenic propane. Based on our model evaluations Type I and II kerogens contain similar fraction of both precursors, and precursor B is more abundant by about 10% than precursor A. This indicates that a stronger enrichment of ^{13}C at central carbon positions of propane isotopologues. Moreover, the two precursors are carrying different original carbon isotopic signatures, and the maximum difference is about 5.8‰ (see Table 1). Notably, the predicted bulk carbon isotopic signatures of Type I and II kerogens are the weighted mean of precursor A and precursor B, and are consistent with the measured bulk carbon isotopic signatures of different source materials. This demonstrates that the simulated initial fraction and carbon isotopic signatures of the different precursors are valid.

Based on the same model and parameters optimized for kerogen I ,we conducted scenario modeling by adjusting initial content of different precursors (0% to 100%) in order to investigate how initial fraction of precursor A and precursor B could influence obtained $\delta^{13}C_a$ and $\delta^{13}C_b$ signals. As shown in Figure 4, the darker lines represent higher initial fraction of precursor A, resulting in a horizontal line at 100% precursor A. This is due to cleavage of carbon atom only at terminal carbon positions via pathway A. The lines are trending vertical accompanied by increasing initial content of precursor B, where propane yield via pathway B is contributing increasingly more. At late reaction time destruction of propane become dominant, and thus resulting in identical carbon isotopic behavior of propane released at different initial conditions. The simulated results indicated that initial fraction of different precursors could significantly influence obtained $\delta^{13}C_a$ and $\delta^{13}C_b$ signals, and meanwhile initial fractions of precursor A and precursor B in a certain kerogen could be characterized and resolved through the observed $\delta^{13}C_a$ and $\delta^{13}C_b$ correlations.

CONCLUSIONS

This study established a mathematical framework to describe reaction network as well as kinetics of position specific carbon isotopologues of thermogenic propane and its precursors, and thus providing a robust approach for mechanistic interpretation of both bulk and position specific carbon isotopic evolution of propane. The simulated results agree well with the experimental data, and thus the modelling approach is validated and ready for different applications. Notably, the model correctly linked the observed PSIA signals with the initial fraction and carbon isotopic signatures of specific precursors in source materials. Thus, our model could serve as a valuable tool to quantify underlying parameters such as source organics isotopic compositions and formation temperature that could impact position specific carbon isotopic evolution of thermogenic propane. Moreover, our model allows integrating more complex reaction mechanisms to elucidate unknown reaction pathways as well as to guide and optimize future experimental studies for testing different hypothesis.

REFERENCES

1. Stolper, D.A., Lawson, M., Davis, C.L., et al. (2014). Formation temperatures of thermogenic and biogenic methane. Science **344**(6191): 1500–1503. DOI: 10.1126/science.1254509.
2. Schoell, M. (1988). Multiple origins of methane in the Earth. Chemical Geology **71**(1): 1–10. DOI: 10.1016/0009-2541(88)90101-5.
3. Dai, J., Zou, C., Liao, S., et al. (2014). Geochemistry of the extremely high thermal maturity Longmaxi shale gas, southern Sichuan Basin. Organic Geochemistry **74**: 3–12. DOI: 10.1016/j.orggeochem.2014.01.018.
4. Queneau, Y., and Han, B. (2022). Biomass: Renewable carbon resource for chemical and energy industry. The Innovation **3**(1): 100184. DOI: 10.1016/j.xinn.2021.100184.
5. Zhang, X. (2023). Uncover the black box of black shales. The Innovation Geoscience **1**(1): 100005. DOI: 10.59717/j.xinn-geo.2023.100005.
6. Gilbert, A., Sherwood Lollar, B., Musat, F., et al. (2019). Intramolecular isotopic evidence for bacterial oxidation of propane in subsurface natural gas reservoirs. Proceedings of the National Academy of Sciences **116**(14): 6653–6658. DOI: 10.1073/pnas.1817784116.
7. Gilbert, A. (2021). The Organic Isotopologue Frontier. Annual Review of Earth and Planetary Sciences **49**(1): 435–464. DOI: 10.1146/annurev-earth-071420-053134.
8. Gao, L., He, P., Jin, Y., et al. (2016). Determination of position-specific carbon isotope ratios in propane from hydrocarbon gas mixtures. Chemical Geology **435**: 1–9. DOI: 10.1016/j.chemgeo.2016.04.019.
9. Li, Y., Zhang, L., Xiong, Y., et al. (2018). Determination of position-specific carbon isotope ratios of propane from natural gas. Organic Geochemistry **119**: 11–21. DOI: 10.1016/j.orggeochem.2018.02.007.
10. Piasecki, A., Sessions, A., Lawson, M., et al. (2016). Analysis of the site-specific carbon isotope composition of propane by gas source isotope ratio mass spectrometer. Geochimica et Cosmochimica Acta **188**: 58–72. DOI: 10.1016/j.gca.2016.04.048.
11. Zhang, L., Li, Y., Jiang, W., and Xiong, Y. (2022). Position-specific carbon isotopic composition of thermogenic propane: Insights from pyrolysis experiments. Organic Geochemistry **166**: 104379. DOI: 10.1016/j.orggeochem.2022.104379.
12. Piasecki, A., Sessions, A., Lawson, M., et al. (2018). Position-specific 13C distributions within propane from experiments and natural gas samples. Geochimica et Cosmochimica Acta **220**: 110–124. DOI: 10.1016/j.gca.2017.09.042.
13. Piasecki, A., Sessions, A., Peterson, B., and Eiler, J. (2016). Prediction of equilibrium distributions of isotopologues for methane, ethane and propane using density functional theory. Geochimica et Cosmochimica Acta **190**: 1–12. DOI: 10.1016/j.gca.2016.06.003.
14. Gilbert, A., Yamada, K., Suda, K., et al. (2016). Measurement of position-specific 13C isotopic composition of propane at the nanomole level. Geochimica et Cosmochimica Acta **177**: 205–216. DOI: 10.1016/j.gca.2016.01.017.
15. Chung, H.M., Gormly, J.R., and Squires, R.M. (1988). Origin of gaseous hydrocarbons in subsurface environments: Theoretical considerations of carbon isotope distribution. Chemical Geology **71**(1): 97–104. DOI: 10.1016/0009-2541(88)90108-8.
16. Tang, Y., Perry, J.K., Jenden, P.D., and Schoell, M. (2000). Mathematical modeling of stable carbon isotope ratios in natural gases † †We dedicate this paper to Bill Sackett on the occasion of his 70th birthday. Geochimica et Cosmochimica Acta **64**(15): 2673–2687. DOI: 10.1016/S0016-7037(00)00377-X.
17. Rooney, M.A., Claypool, G.E., and Moses Chung, H. (1995). Modeling thermogenic gas

generation using carbon isotope ratios of natural gas hydrocarbons. Chemical Geology **126**(3): 219–232. DOI: 10.1016/0009-2541(95)00119-0.
18. Xie, H., Dong, G., Formolo, M., et al. (2021). The evolution of intra- and inter-molecular isotope equilibria in natural gases with thermal maturation. Geochimica et Cosmochimica Acta **307**: 22–41. DOI: 10.1016/j.gca.2021.05.012.
19. Jin, B., and Rolle, M. (2016). Position-specific isotope modeling of organic micropollutants transformation through different reaction pathways. Environmental Pollution **210**: 94–103. DOI: 10.1016/j.envpol.2015.11.014.
20. Jin, B., and Rolle, M. (2014). Mechanistic approach to multi-element isotope modeling of organic contaminant degradation. Chemosphere **95**: 131–139. DOI: 10.1016/j.chemosphere.2013.08.050.
21. Maggi, F., and Riley, W.J. (2010). Mathematical treatment of isotopologue and isotopomer speciation and fractionation in biochemical kinetics. Geochimica et Cosmochimica Acta **74**(6): 1823–1835. DOI: 10.1016/j.gca.2009.12.021.
22. Xie, H., Formolo, M., and Eiler, J. (2022). Predicting isotopologue abundances in the products of organic catagenesis with a kinetic Monte-Carlo model. Geochimica et Cosmochimica Acta **327**: 200–228. DOI: 10.1016/j.gca.2022.03.028.
23. Jin, B., Laskov, C., Rolle, M., and Haderlein, S.B. (2011). Chlorine Isotope Analysis of Organic Contaminants Using GC–qMS: Method Optimization and Comparison of Different Evaluation Schemes. Environmental Science & Technology **45**(12): 5279–5286. DOI: 10.1021/es200749d.
24. Jin, B., Haderlein, S.B., and Rolle, M. (2013). Integrated Carbon and Chlorine Isotope Modeling: Applications to Chlorinated Aliphatic Hydrocarbons Dechlorination. Environmental Science & Technology **47**: 1443–1451. DOI: 10.1021/es304053h.

ACKNOWLEDGMENTS

This work was supported by Guangdong Foundation for Science and Technology Research (2023B1212060049). We are grateful to Prof. Jinzhong Liu, Dr. Yun Li and Dr. Wenmin Jiang for their helpful discussions on the kerogen cracking experiments and the experimental data for model validation.

AUTHOR CONTRIBUTIONS

P.P. and B.J. designed the study; B.J. developed mathematical framework and conducted simulations; P.P. analyzed the simulation results; B.J. wrote the manuscript under P.P.'s supervision.

DECLARATION OF INTERESTS

The authors declare no competing interests.

SUPPLEMENTAL INFORMATION

It can be found online at https://doi.org/10.59717/i.xinn-geo.2024.100054

LEAD CONTACT WEBSITE

Biao Jin: https://www.researchgate.net/profile/Biao-Jin